

Explicit Correction for Material Motion in Radiative Transport

D.B. Carrington,* S.A. Turner*

*Los Alamos National Laboratory, Los Alamos, New Mexico 87545

In this paper, we present comparisons of the solutions to the partial differential equations modeling radiative transport in moving media with constant velocity field to a quasi-analytic transport solution for plane-parallel media. We also perform verification of a finite volume discretization for the gray approximation to radiative transfer in media having low velocity (1 to 2% the speed of light). We present the discretizations and the nonlinear solution algorithm for radiative transfer in moving media using an explicit energy-update. In a previous article, we discussed other formulations compared to the explicit-update formulation (Carrington and Turner, 2004). The focus here is on the explicit-energy update system.

Incorporating velocity correction terms to order $\mathcal{O}(v/c)$ in the radiative transfer equations produces results having good agreement to the quasi-analytic transport solution for material with low velocity. A symmetrical system of equations is maintained by incorporating the divergence of material motion flux on the right-hand side; the energy-split method lags the divergence of the flux associated with material motion $\frac{4}{3}\bar{v}E_{\text{face}}$ in the nonlinear iteration. Not incorporating any velocity correction terms in the transfer solution also produces good agreement with the quasi-analytic transport solution since the correction terms are small at the velocities in the comparisons where the assumptions are valid. However, there are small differences between the solutions that use and do not use material-motion correction.

Making comparisons to validate the method is difficult since the analytic solution is providing the transfer/diffusion solution with boundary values. These boundary conditions for the transfer solution are determined by the quasi-analytic transport problem; the solution is constrained to a given regime. When thermo-fluid processes are determining the dynamics, greater differences between the velocity-corrected and uncorrected solutions should exist.

Introduction

Approximating radiative transport by first-order spherical harmonic equations produces a zeroth-order energy equation, which, when integrated over all frequencies (gray equations), is

$$\frac{1}{c} \frac{\partial E}{\partial t} + \frac{1}{c} \nabla \cdot \bar{\mathbf{F}} = \sigma_a \left[aT_r^4 - E \right]. \quad [1]$$

The gray first moment, or angular momentum of the transfer equation is

$$\frac{\eta}{c} \frac{\partial \bar{\mathbf{F}}}{\partial t} + c \nabla \cdot \frac{1}{3} \bar{\bar{\mathbf{E}}} = -\sigma_t \bar{\mathbf{F}}, \quad [2]$$

where σ_a and σ_t are absorption and total opacities, respectively. The first moment closure for the radiation pressure is given by $\bar{\bar{\mathbf{P}}} = \frac{1}{3} \text{diag}(\bar{\bar{\mathbf{E}}})$ (isotropic field), and η is 1, $\frac{1}{3}$, or 0 for either the P_1 , $P_{1/3}$, or diffusion approximation, respectively. These equations are for stationary material.

Consideration for material motion relative to the inertial frame is accomplished to an order of accuracy $\mathcal{O}(v/c)$ when the opacities and material coefficients are evaluated in the co-moving frame. Adding a velocity correction term to the radiative energy transfer equations (Mihalas and Klein, 1982) results in the mixed-frame equation

$$\frac{1}{c} \frac{\partial E}{\partial t} + \frac{1}{c} \nabla \cdot \bar{\mathbf{F}} = \sigma_a \left[aT_r^4 - E \right] - \frac{\sigma_t}{c^2} \bar{\mathbf{v}} \cdot \bar{\mathbf{F}}_o, \quad [3]$$

where $\bar{\mathbf{v}}$ is the velocity vector, and, defining the Lagrangian frame variables,

$$\bar{\mathbf{F}}_o = \bar{\mathbf{F}} - \frac{4}{3} \bar{\mathbf{v}} E^n \quad \text{and} \quad E_o = E - 2 \frac{\bar{\mathbf{v}}}{c^2} \cdot \bar{\mathbf{F}}_o. \quad [4]$$

A formulation using an explicit-energy update only requires averaging face or edge quantities for those values that reside at the cell-center, e.g., terms associated with the Planck mean opacity σ_a . Equation [4] is precisely the Lorentz transformation of Eulerian frame to the Lagrangian or co-moving frame (Mihalas and Mihalas, 1984).

Using energies calculated at the cell faces where possible results in an energy density equation given by

$$\frac{1}{c} \frac{\partial E}{\partial t} + \frac{1}{c} \nabla \cdot \left(\bar{\mathbf{F}}_o + \bar{\mathbf{v}} \frac{4}{3} E_{\text{face}} \right) = \sigma_a \left[aT^4 - E + 2 \frac{\bar{\mathbf{v}}}{c^2} \cdot (\bar{\bar{\mathbf{F}}}_o) \right] - \frac{\sigma_t}{c^2} \bar{\mathbf{v}} \cdot (\bar{\mathbf{F}}_o), \quad [5]$$

where \bar{v} is averaged to the cell center for each coordinate direction. For the product term $\bar{v} \cdot \bar{F}$, \bar{F} is also averaged from the face values.

The flux equation is solved (as per Morel, 2004) in the Lagrangian frame

$$\bar{F}_o^{l+1} = -\omega D_i^l n \cdot \nabla E^{l+1} + (1 - \varpi) \bar{F}_o^l, \quad [6]$$

and, transforming to the Eulerian frame, it becomes

$$\bar{F}^{n+1} = \bar{F}_o^{n+1} + \frac{4}{3} \bar{v} E_{face}^{n+1}. \quad [7]$$

The Eulerian flux is in the divergence operation of equation [5], and has drift term $\frac{4}{3} \bar{v} E_{face}$.

Other discretizations are possible; the results of some were presented in the previous article (Carrington and Turner, 2004).

Material Energy

The equation for material energy includes exchange between the radiation field and the material temperature field. This equation, including the application of a velocity correction term, is

$$C_v \frac{\partial T}{\partial t} = Q - c \sigma_a \left(a T^4 - E + 2 \frac{\bar{v} \cdot \bar{F}_o}{c^2} \right), \quad [8]$$

where Q is the material energy source term, and C_v is the material specific heat capacity.

Momentum Deposition Discretization

The change in momentum from photon interaction with the material is given by

$$d(m\bar{v}) = v dm + m dv = m dv = m(v^{n+1} - v^n). \quad [9]$$

For a constant density material, this equation is

$$d(m\bar{v}) = m(\bar{v}^{n+1} - \bar{v}^n) = m\bar{a} dt, \quad [10]$$

where

$$m\bar{a} dt = Vol \frac{\sigma_i \bar{F}^{n+1}}{c} dt, \quad [11]$$

which is the vector for photon momentum deposition that is added to the material momentum.

Time Integration and Fixed-Point Iteration for Incorporating Nonlinearity

Utilizing a fixed-point iteration addresses the nonlinear behavior of the equations. This fixed-point method progresses in a split process: energy, radiation flux, radiation exchange to the material, and then heat conductance in the material. The exchange terms are not considered a split, since the method incorporates the implicit temperature in the energy equation and the implicit energy in the temperature equation—an algebraic equivalent system as shown in equations [16] through [21]. A split is actually present at the solution for the effects of thermal conductance.

Complications arise from both the nonlinearity introduced from temperature-dependent material properties and from a poor estimate of T^* used to linearize T^4 . The nonlinearities at each time step must be converged before advancing another time step, i.e.,

$$\left| \frac{T^{l+1} - T^l}{T^{l+1}} \right| < \varepsilon, \quad [12]$$

where l is the iteration level. This fixed-point method provides some assurance that the correct opacities are being used to calculate the energy density. It does not assure that the time integration is accurate.

Discrete Equations

The equation for energy density—including the linearization of T^4 by a Taylor expansion around some intermediate value T^* between T^n and T^{n+1} and assuming a diffusion approximation—is given by

$$\frac{1}{c} \frac{\partial E}{\partial t} + \frac{1}{c} \nabla \cdot D \nabla \frac{E}{3} = \sigma_a \left[a T_e^{*3} (4 T_e^{n+1} - 3 T_e^*) - E + 2 \frac{\bar{v}}{c^2} \cdot \left(\bar{F} - \bar{v} \frac{4}{3} E \right) \right] - \frac{\sigma_t}{c^2} \bar{v} \cdot \left(\bar{F} - \bar{v} \frac{4}{3} E \right). \quad [13]$$

After combining like terms and averaging vector-valued quantities to the cell center where appropriate, we find that the energy density in the lab frame is

$$\frac{1}{c} \frac{\partial E}{\partial t} + \frac{1}{c} \nabla \cdot D \nabla \frac{E}{3} = \sigma_a \left[a T_e^{*3} (4 T_e^{n+1} - 3 T_e^*) - E \right] + 2 \sigma_a \frac{\bar{v}}{c^2} \cdot \bar{F}_0 - \sigma_t \frac{\bar{v}}{c^2} \cdot \bar{F}_0. \quad [14]$$

The explicit ordinary differential equation for material temperature is given by

$$C_v \frac{\partial T}{\partial t} = Q - c \sigma_a \left(a T_e^{*3} (4 T_e^{n+1} - 3 T_e^*) - E^{n+1} + 2 \frac{\bar{v} \cdot \bar{F}_0}{c^2} \right), \quad [15]$$

where units are appropriately applied for the application that best suits the energy and time scales.

The equations in their discrete and algorithmic form are derived by starting with the determination of the $l+1$ iterate for material temperature, given as

$$T^{l+1} = \frac{C_v^l}{c dt \left(\frac{C_v^l}{c dt} + 4\sigma_a^l a T_e^{*3} \right)} T^n + \frac{\sigma_a \left[E^{l+1} - 3a T_e^{*4} \right]}{\frac{C_v^l}{c dt} + 4\sigma_a^l a T_e^{*3}} - 2\sigma_a^l \frac{\bar{v}}{c^2} \cdot \bar{F}_o^l. \quad [16]$$

This first-order ordinary differential equation only requires current (or initial) conditions for solution for cell-centered values. Updating vertex valued fields, e.g., applying a finite-element method, would take special consideration for conditions at the boundary.

Substituting this temperature into equation [13] produces a system of equations that is algebraically equivalent to an implicit solution method. The discrete equation is given by

$$\begin{aligned} Vol_{cell} \left[\frac{1}{c dt} + \sigma_a^l - \frac{4a\sigma_a^l T_e^{*3}}{\frac{C_v^l}{c dt} + 4\sigma_a^l a T_e^{*3}} \right] E^{l+1} + \sum_{i=1}^{\#faces} A_i \hat{n} \cdot \bar{F}_i^{l+1} &= Vol_{cell} \frac{E^n}{c dt} + \\ Vol_{cell} \sigma_a^l T_e^{*3} \left[\frac{4aC_v^l}{c dt \left(\frac{C_v^l}{c dt} + 4\sigma_a^l a T_e^{*3} \right)} T_e^n + \frac{12a^2 \sigma_a^l T_e^{*4}}{\left(\frac{C_v^l}{c dt} + 4\sigma_a^l a T_e^{*3} \right)} - 3T_e^* \right] &- \\ Vol_{cell} \left[\frac{4a\sigma_a^l \bar{F}^{l,l}}{\frac{C_v^l}{c dt} + 4\sigma_a^l a T_e^{*3}} + 2\sigma_a^l \frac{\bar{v}}{c^2} \cdot \bar{F}_o^l - \sigma_a^l \frac{\bar{v}}{c^2} \cdot \bar{F}_o^l \right]. & \end{aligned} \quad [17]$$

The first moment, or angular moment of the transfer equation is

$$\frac{\eta}{c} \frac{\bar{F}^{l+1} - \bar{F}^n}{dt} + \frac{c}{3} \bar{\nabla} E^l = \sigma_a^l \bar{F}_o^l. \quad [18]$$

Using the diffusion approximation with the flux given by Fick's Law,

$$\bar{F}^{l+1} = \frac{c}{3\sigma_a^l} \bar{\nabla} E^{l+1}, \quad [19]$$

the energy density equation (Knoll et al, 2001) becomes

$$\begin{aligned}
 & \left(\frac{1}{cdt} + \sigma_a^l - \frac{4a\sigma_a^l T_e^{*3}}{\frac{C_v^l}{cdt} + 4\sigma_a^l a T_e^{*3}} \right) E^{l+1} + \frac{\sum_{i=1}^{\# \text{ faces}} \left(A_i D_i^l \hat{n} \cdot \bar{\nabla} E_c^{l+1} \right)_i}{Vol_{cell}} = \frac{E^n}{cdt} + \\
 & \sigma_a^l T_e^{*3} \left[\frac{4aC_v^l}{cdt \left(\frac{C_v^l}{cdt} + 4\sigma_a^l a T_e^{*3} \right)} T_e^n + \frac{12a^2 \sigma_a^l T_e^{*4}}{\left(\frac{C_v^l}{cdt} + 4\sigma_a^l a T_e^{*3} \right)} - 3T_e^* \right] - \\
 & \left[\frac{4a\sigma_a^l \bar{F}^{l,l}}{\frac{C_v^l}{cdt} + 4\sigma_a^l a T_e^{*3}} + 2\sigma_a^l \frac{\bar{v}}{c^2} \cdot \bar{F}_o^l - \sigma_a^l \frac{\bar{v}}{c^2} \cdot \bar{F}_o^l \right].
 \end{aligned} \tag{20}$$

In equation [20], $D_i^l = \frac{c}{3\sigma_i^l}$ is for the i^{th} face, the gradient of the cell energy, and $\bar{\nabla} E_c$ is the gradient of energy across the cell as determined by the calculation of energy at the faces found using Fick's Law.

The conduction equation is given as

$$C_v^l \frac{T^{l+1} - T^n}{dt} = \nabla \cdot \mathbf{k}^l \nabla T^l. \tag{21}$$

Boundary conditions for this equation are either Neumann or Dirichlet.

Boundary Conditions

First-order spherical harmonics equations require a single boundary condition for the equations for energy density and flux at the boundary surface—a boundary condition to satisfy both the zeroth- and first-moment equations. Also, two other equations—the equation describing radiative energy exchange to the material and heat conduction in the material, and the equation describing the exchange between the ionized plasma—require boundary conditions.

The required boundary conditions for radiative transfer can be accomplished with

$$\int_{n \cdot \Omega} \left[\frac{c}{4\pi} E(r, \nu, t) - \frac{3}{4\pi} \Omega \cdot \bar{F}(r, \nu, t) \right] \hat{n} \cdot \Omega d\Omega = \int_{n \cdot \Omega} \Gamma(r, \nu, \Omega, t) \hat{n} \cdot \Omega d\Omega, \tag{22}$$

which satisfies the transfer equation in an integral sense. The term $\int_{n \cdot \Omega} \Gamma(r, \nu, \Omega, t) \hat{n} \cdot \Omega d\Omega$ is some incoming distribution of radiation, and \hat{n} is the outward normal vector to the

surface. This equation is the Marshak boundary condition. After the left-hand side of equation [22] is integrated, the boundary statement is

$$\frac{c}{4} E(r, \nu, t) - \frac{1}{2} \hat{n} \cdot \bar{F}(r, \nu, t) = \int_{n \cdot \Omega} \Gamma(r, \nu, \Omega, t) \hat{n} \cdot \Omega d\Omega. \quad [23]$$

When consideration for material motion is made for time-independent boundaries and when we have integrated over frequency and the surface, this Marshak-type radiative boundary condition is expressed as

$$\frac{c}{4} E_b - \frac{1}{2} \hat{n} \cdot \bar{F}_{ob} = \Gamma. \quad [24]$$

A Marshak boundary condition can be implemented by the function

$$\alpha E + \beta \hat{n} \cdot \bar{F}_o = f_{bf}, \quad [25]$$

where $\alpha = c/4$, $\beta = \frac{1}{2D}$, $n \cdot \bar{F}_o = D \frac{\partial E}{\partial n}$, and f_{bf} is the given value of the function at the face. This is a Robin-type boundary condition. It is different from the type generally referred to in the field of hydrodynamics. If $f_{bf} = 0$, a vacuum condition, the boundary integral is

$$\frac{c}{4} E - \frac{1}{2} \hat{n} \cdot \bar{F}_{ob} = 0. \quad [26]$$

If $f_{bf} = \frac{cE_b}{4}$, then a reflective boundary is produced, yielding

$$\hat{n} \cdot \bar{F}_{ob} = 0 \Rightarrow \bar{F} = \frac{4}{3} \bar{\nu} E_b. \quad [27]$$

Note: This situation can be specified by assigning $\alpha = 0$ and $f_{bf} = 0$. If a radiation intensity (energy density) is applied at the surface, the flux is calculated directly from Fick's Law, and the Marshak condition becomes, after substitution for \bar{F}' is made from equation [4],

$$\frac{c}{4} E_b - \frac{1}{2} \hat{n} \cdot \left(A_b D_b' \frac{E_b - E_c^{l+1}}{ds} - \frac{4}{3} \bar{\nu} E_b^n \right) = 0. \quad [28]$$

The energy equation for Newtonian fluids (in which enthalpy is presumed to be a function of pressure and temperature) can be stated as

$$C_v \frac{\partial T}{\partial t} = Q - c\sigma_a \left(aT^4 - E + 2 \frac{\bar{\mathbf{v}} \cdot \bar{\mathbf{F}}_o}{c^2} \right) + \nabla \cdot \mathbf{k} \nabla T + \bar{\mathbf{v}} \cdot \nabla T. \quad [29]$$

In this equation, ‘k’ is the electron conductance. The boundary conditions are either Neumann or Dirichlet conditions.

The Neumann boundary condition is a given flux at the surface

$$q_b = k \frac{\partial T}{\partial \hat{n}}, \quad [30]$$

where

$$\frac{\partial T}{\partial n} = \hat{n} \cdot \nabla T = n_x \frac{\partial T}{\partial x} + n_y \frac{\partial T}{\partial y}. \quad [31]$$

The direction cosines n_x and n_y are obtained from noticing that $n_x = \cos \phi = \frac{dy}{d\Gamma}$, and $n_y = \sin \phi = -\frac{dx}{d\Gamma}$.

Solution Method—Explicit Update to Correct for Material Motion

The Eulerian-frame formulation for the energy variables, combined with the co-moving frame material properties, makes for a “mixed-frame” equation set. The general development of these equations is described in Mihalas and Mihalas (1984).

Updating energy density with face-based values in an explicit second step uses mostly unaltered coding to solve equation [1]. It is assumed that most coding errors can be avoided with the explicit statement by *tacking-on* the material-motion correction terms to the original code. This method also helps to isolate terms associated with material motion flux.

Temperature and Energy Density

Starting with the “corrected” material temperature

$$T^{l+1} = \frac{\frac{C_v^l}{dt} T^n + 3c\sigma_a^l aT^{*4} + c\sigma_a^l E^{l+1} - 2\sigma_a^l \bar{\mathbf{v}} \cdot \bar{\mathbf{F}}_o^l}{\frac{C_v^l}{dt} + 4c\sigma_a^l aT^{*3}}, \quad [32]$$

and, as before, substituting material temperature in the equation for photon energy density produces

$$\begin{aligned}
 & \frac{1}{c} \left[\frac{E^{l+1/2} - E^n}{dt} - \frac{\sum_{i=1}^{\# \text{ faces}} A_i (\omega D_i^l \hat{n} \cdot \nabla E^{l+1} - (1 - \varpi) \bar{F}_o^l)_i}{Vol} \right] - \frac{4\sigma_a^l E^{l+1}}{\frac{C_v^l}{dt} + 4ca\sigma_a^l T^{*3}} + \sigma_a^l E^{l+1} = \\
 & \sigma_a^l T^{*3} \left[\frac{4 \frac{C_v^l}{cdt} T^n + 12\sigma_a^l a T^{*4} - \frac{8\sigma_a^l \bar{v} \cdot \bar{F}_o^l}{c}}{\frac{C_v^l}{dt} + 4ca\sigma_a^l T^{*3}} \right] - 3\sigma_a^l a T^{*4} + 2\sigma_a^l \frac{\bar{v} \cdot \bar{F}_o^l}{c^2}
 \end{aligned} \tag{33}$$

where $\varpi = \frac{c\sigma_t^l dt}{\eta + c\sigma_t^l dt}$ and η is either 1 or 1/3 for P₁ and P_{1/3}, respectively, (for diffusion $\varpi = 1$). The amount of lagged radiation flux in equation [33] is determined by the value of ω , which is derived from incorporating time-dependent flux in the following manner:

$$\frac{1}{c} \left[\frac{E^{l+1} - E^{l+1/2}}{dt} \right] = -\sigma_t^l \frac{\bar{v} \cdot \bar{F}_o^l}{c^2} - \nabla \cdot \frac{4}{3} \bar{v} E_{edge}^l. \tag{34}$$

Performing the divergence in equation [34] yields

$$Vol \frac{1}{c} \left[\frac{E^{l+1} - E^{l+1/2}}{dt} \right] = -\sigma_t^l \frac{\bar{v} \cdot \bar{F}_o^l}{c^2} - \frac{\sum_{i=1}^{\# \text{ faces}} A_i \hat{n} \cdot \frac{4}{3} \bar{v} E_{edge}^l}{Vol}. \tag{35}$$

Flux

The first part of the flux is determined by

$$\bar{F}_o^{l+1} = -\omega D_i^l n \cdot \nabla E^{l+1} + (1 - \varpi) \bar{F}_o^n. \tag{36}$$

and is used in the divergence term of the first half-step energy calculation, where \bar{F}_o^l on the right-hand side is the co-moving-frame flux from the previous iteration. The $l+1^{\text{st}}$ flux, the lab-frame flux, is

and this equation simply determines the flux in Eulerian frame

$$\bar{F}^{l+1} = -\omega D_i^l n \cdot \nabla E^{l+1} + (1 - \varpi) \bar{F}_o^{l+1} + \frac{4}{3} \bar{v} E_{face}^l. \tag{37}$$

The explicit-update formulation moves the divergence of the vector quantity for $\bar{v} E_{face}^l$ to the right-hand side of equation [33] in a second step as given by equation [35]. This method requires a couple of iterations for convergence, but considering the time and

complexity for construction of the entire Eulerian frame flux on the left-hand side of equation [33], the extra cost seems a small price to pay, particularly since the nonlinearity is opacity is requiring iteration.

Analytic Validation of Mixed-Frame Diffusion Approximation

It is possible to generate test problems in both the Cartesian and spherically symmetric coordinates. This study will make a comparison to quasi-analytic solutions for plane-parallel media. The quasi-analytic solution is developed in the following section. The details of the numerical integration are handled by MathCad software (www.mathcad.com). The coding for the quasi-analytic solution is presented in Carrington and Turner, 2004.

Plane-Parallel Media Moving at Constant Velocity

A transport method is used to evaluate the intensity within the media and is determined by

$$\mu \frac{\partial I}{\partial \tau} = \gamma(1 - \mu\beta)(\sigma_a + \sigma_s) \left[-I(\tau) + \left(1 - \frac{\sigma_a}{\sigma_a + \sigma_s}\right)J(\tau) + \frac{\sigma_a}{\sigma_a + \sigma_s} B(\tau) \right], \quad [38]$$

where $\gamma = \frac{1}{(1 - \beta^2)^{1/2}}$, and $\beta = \frac{\bar{v}}{c}$. In terms of a de-excitation coefficient, $\lambda = \frac{\sigma_a}{\sigma_t}$, and $\sigma_t = \sigma_a + \sigma_s$ in equation [38]. The resulting equation (Pistner and Shaviv, 1994), can be written as

$$\mu \frac{\partial I}{\partial \tau} = \gamma(1 - \mu\beta)\sigma_t \left[-I(\tau) + (1 - \lambda)J(\tau) + \lambda B(\tau) \right]. \quad [39]$$

Integrating over the solid angle for the gradient flux,

$$\frac{\partial F}{\partial \tau} = \int_{\Omega} \mu \frac{\partial I}{\partial \tau} d\Omega. \quad [40]$$

In planar atmospheres, homogenous in x and y, only F_z is nonzero,

$$F_z = 2\pi \int_{-1}^1 I(z, \mu) \mu d\mu, \quad [41]$$

and

$$\frac{\partial F_z}{\partial \tau} = 2\pi \int_{-1}^1 I(z, \mu) \mu d\mu. \quad [42]$$

The flux associated with a plane wave is constant in the local equilibrium limit and in the co-moving frame. Performing the integration,

$$\begin{aligned} \frac{1}{2} \int_{-1}^1 \frac{\partial I(z, \mu)}{\partial \tau} \mu d\mu &= \frac{1}{2} \gamma \left[\int_{-1}^1 -I d\mu + \int_{-1}^1 J d\mu - \lambda \int_{-1}^1 J d\mu + \int_{-1}^1 I_b d\mu \right] + \\ &\frac{1}{2} \gamma \left[\int_{-1}^1 \beta I \mu d\mu - \int_{-1}^1 \beta J \mu d\mu + \int_{-1}^1 \beta \lambda J \mu d\mu - \int_{-1}^1 \beta \lambda I_b \mu d\mu \right]. \end{aligned} \quad [43]$$

Canceling terms in equation [43] results in the spatial derivative of Eddington flux

$$\frac{\partial F}{\partial \tau} = -\gamma \beta F [1 - 2\lambda]. \quad [44]$$

Integrating the Eddington flux over optical thickness produces

$$F = c e^{-\int_0^{\tau_0} (1-2\lambda) \beta d\tau}. \quad [45]$$

The mean intensity is determined from the relation

$$\frac{\partial J}{\partial \tau} = 3F. \quad [46]$$

Incorporating the second-moment relation as given in Eddington notation (Mihalas, 1979),

$$K = \frac{1}{2} \int_{-1}^1 I \mu \mu d\mu \Rightarrow J = 3K. \quad [47]$$

This relation for K is substituted into equation [46] to yield

$$\frac{\partial K}{\partial \tau} = \frac{1}{3} \frac{\partial J}{\partial \tau} = \gamma \left[-F + \beta K - \frac{1}{3} \beta J + \frac{1}{3} \beta \lambda J - \frac{1}{3} \beta \lambda I_b \right], \quad [48]$$

which implies that

$$\frac{\partial J}{\partial \tau} = -3\gamma F - \gamma \beta J (\lambda - 1) + 2\gamma \beta^2 \lambda F. \quad [49]$$

Assuming that $\gamma \cong 1$ and dropping higher order $\mathcal{O}(v^2/c^2)$ terms, we get

$$\frac{\partial J}{\partial \tau} = -3\gamma F. \quad [50]$$

Solving the ordinary differential equation [50] for the mean intensity,

$$J = 3F(\tau = 0) \left[1 + \int_0^\tau e^{-\int_0^{\tau'} (1-2\lambda') \beta' d\tau'} d\tau'' \right]. \quad [51]$$

Therefore, after the substitution of J and I_b , the equation for intensity becomes

$$I = 3F(\tau = 0) \left[1 + \int_0^\tau e^{-\int_0^{\tau'} (1-2\lambda(\tau')) \beta(\tau') d\tau'} d\tau'' + \int_0^1 \mu e^{-\int_0^{\tau'} (1-2\lambda(\tau')) \beta(\tau') d\tau'} d\mu \right]. \quad [52]$$

Finally, energy density is determined by the integral of photon intensity over all angles

$$E(\tau) = \frac{1}{4\pi} \int_{-1}^1 I(\tau) d\Omega. \quad [53]$$

The temperature is extracted from the energy-density equation by

$$T(\tau) = \left(\frac{E(\tau)}{ac} \right)^{1/4}.$$

Comparison of the Quasi-Analytic Transport Solution to the Diffusion Approximation

Figures 1 through 8 show the results from a two-temperature radiative transfer calculation at steady state, that is, media in local thermodynamic equilibrium (LTE), for plane-parallel moving media. The numerical results from the radiative transfer software were obtained by setting the interior boundary (at some large optical distance into the media) as a Marshak condition. The surface is a vacuum boundary given by equation [26]. The values at these boundaries were provided by the solution to the quasi-analytic model, the 1-D transport solution described above.

The 1-D transport problem is solved by applying some flux at $\tau = 0$, which scales the problem to a temperature regime. The temperatures at $T(\tau = 0)$ and $T(\tau = \tau_o)$ (where τ_o is some large-mean free path into the body) are the material temperatures at the boundaries in the radiative-transfer solution method. To be precise, the boundary conditions for a two-temperature 2-D radiative-transfer problem are

z-: reflective material at $T(\tau = 0)$ and vacuum radiation (zero Marshak or zero incident flux)

z+: reflective material at $T(\tau = \tau_o)$ and Marshak at material temperature

All other boundary conditions are reflective for both material and radiation.

Figures 1 and 2 show baseline comparisons between the transport solution and the radiative-transfer solution using the diffusion approximation ($\eta = 0$). The percentage difference between the two solutions is also shown in Figure 1 for purely absorbing media and Figure 2 for absorbing and scattering media. There is about a 6% difference at the vacuum boundary for the pure absorber, and the diffusion approximation becomes about 1% at an optical depth of 12.

Augmenting the vacuum boundary by removing the curvature in the energy near the boundary provides better agreement between the diffusion solution and the analytic solution. Adjusting the coefficient on flux (changing its effect) reduces the curvature of the solution except at the boundary. Using d_{eff} in equation [26],

$$\alpha E + \beta \hat{n} \cdot \bar{F}_o = \frac{c}{4} E + \frac{d_{eff}}{2D} \frac{\partial E}{\partial n} = 0, \quad [54]$$

and $d_{eff} = E^*(x_o) \left/ \frac{\partial E}{\partial x_p} \right.$, where E^* is from the Taylor expansion, produces

$$E^*(x_o) = E(x_p) + (x_o - x_p) \frac{\partial E}{\partial x_p}, \quad [55]$$

and effectively changes the significance of the large gradient in energy near the boundary. This operation is performed without changing the boundary temperature.

Depending on the location of point P (a few mean-free paths in depth), the diffusion solution with the augmented boundary condition provides a better match to the transport solution, as shown in Figures 1 and 2. When the material velocity is greater than zero, a numerical adjustment to the boundary condition is not as easy to “fix up,” since the gradient in energy now contains the drift term $4/3 vE$. In any case, diffusion is not a transport solution and does not provide an accurate estimate to the transport equation in optically thin regions.

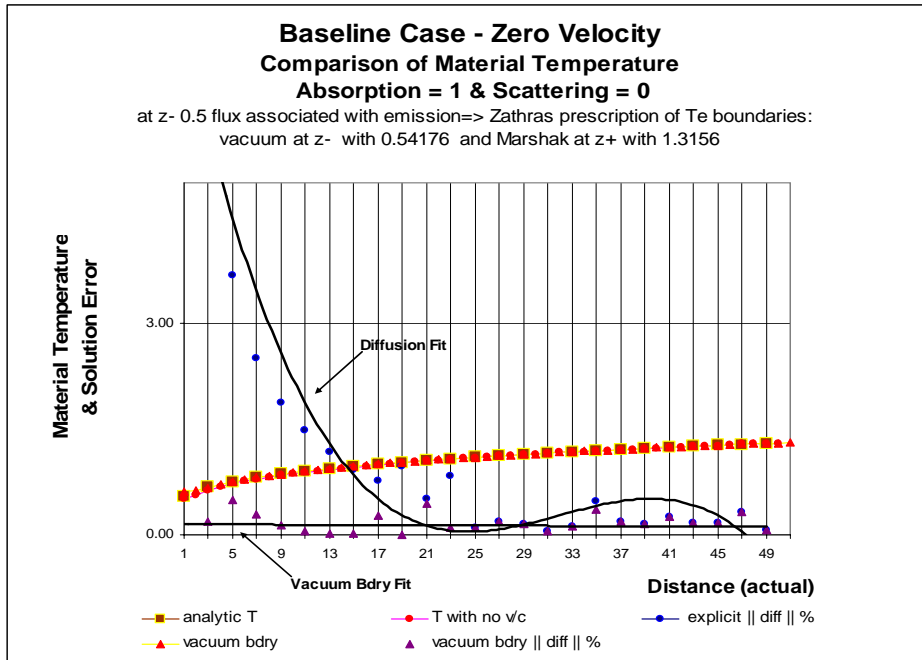


Figure 1. Comparisons of temperature as a function of optical depth in an absorbing material with a zero velocity

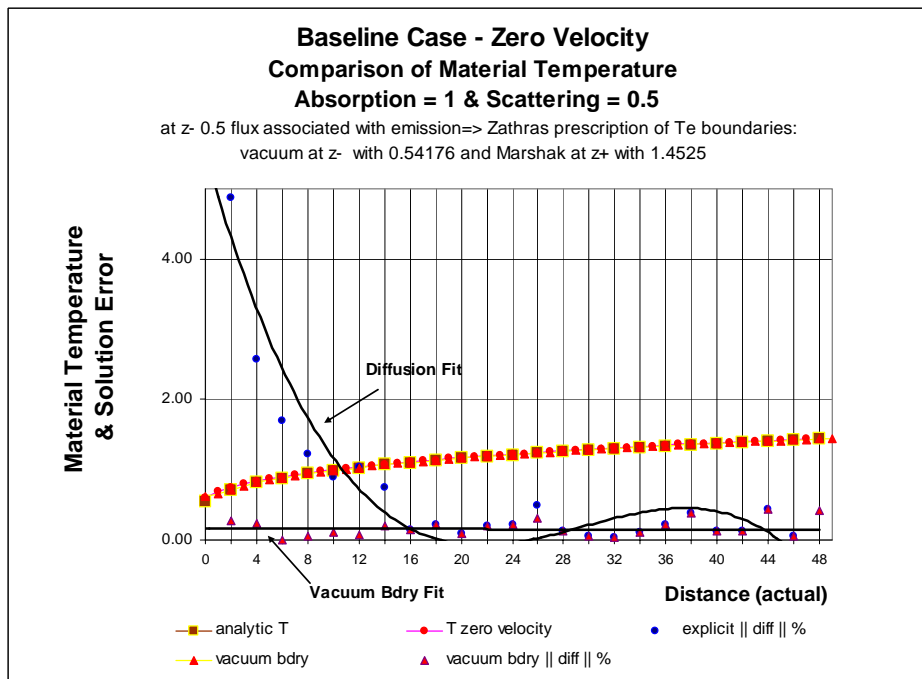


Figure 2. Comparisons of temperature as a function of depth in an absorbing material with a zero velocity

In the next four graphs, four cases are shown at two different velocities, 1% and 2% the speed of light. These cases are:

- purely absorbing media with v/c correction
- purely absorbing media without v/c correction
- scattering and absorbing media with v/c correction
- scattering and absorbing media without v/c correction

The results for these cases are shown in Figures 3 through 7, in which the solutions using correction terms versus solutions without corrections are displayed. There is good agreement for the transfer solution at the Marshak boundary with the quasi-analytic transfer solution for all cases, since the Marshak condition fixes both the energy and the flux. The radiative-transfer solution without correction terms has reasonable agreement with the quasi-analytic solution. At depth, better agreement is achieved with the material-motion correction—perhaps ½% better. Differences are most evident near the vacuum boundary between the solutions. At small depth, the diffusive-type radiative-transfer equations are inaccurate; they are not expected to produce exactly the same answer as a transport solution. The differences (the “error”) at small optical depth are similar to the differences shown in the baseline cases. Calculating T from the energy density magnifies the errors in energy density, since $T = \sqrt[4]{E/a}$ at LTE. Figure 4 shows detail of the differences between the corrected solution and the solution not using correction.

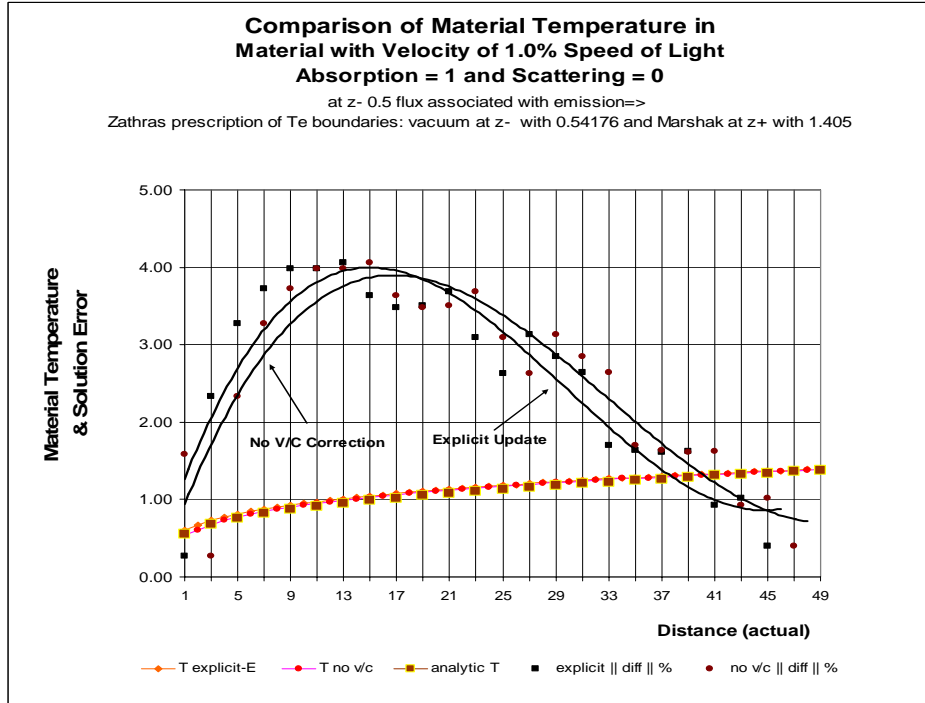


Figure 3. Comparisons of temperature as a function of optical depth in an absorbing material with a velocity of 1% c

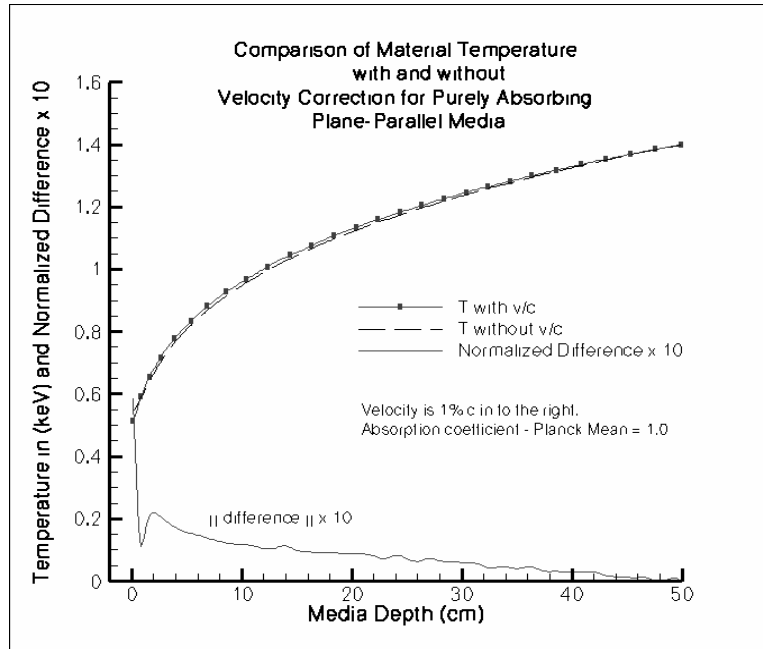


Figure 4. Greater resolution of temperature as a function of optical depth in and absorbing material with and without material-motion correction, media velocity of 1% c

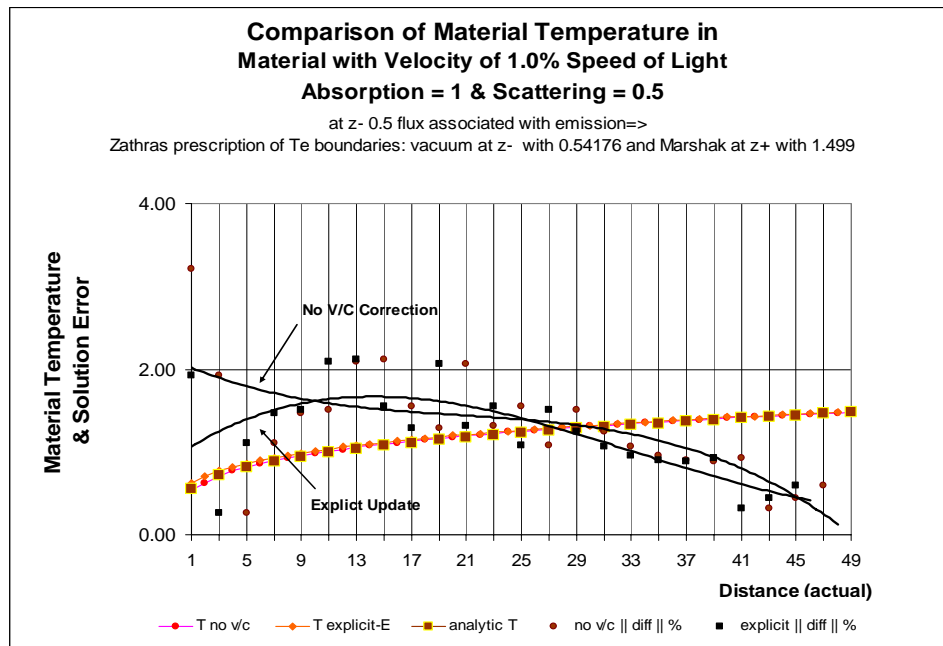


Figure 5. Comparisons of temperature as a function of optical depth in an absorbing and scattering material with a velocity of 1% c

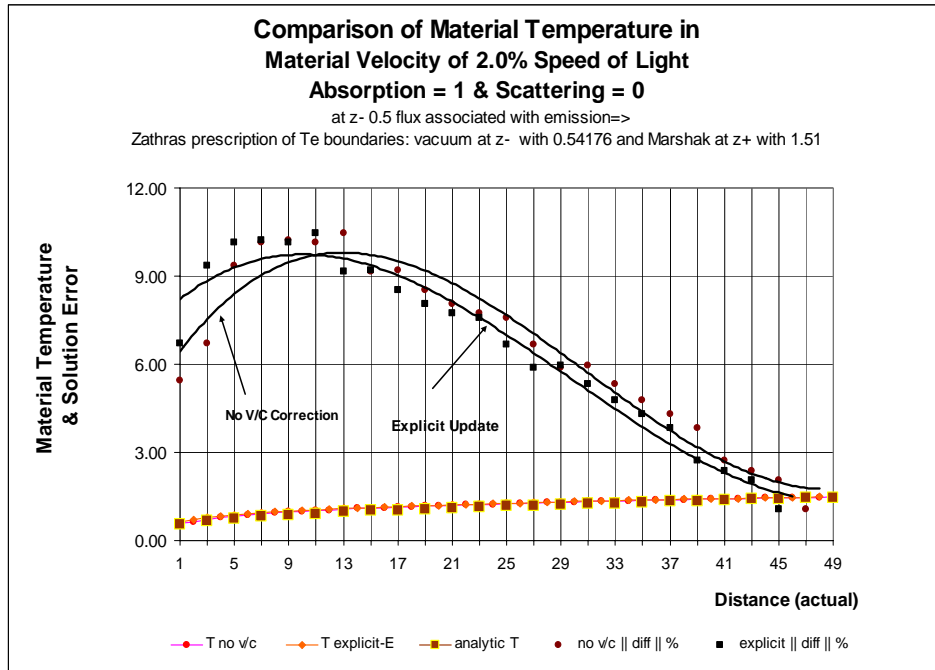


Figure 6. Comparisons of temperature as a function of optical depth in an absorbing material with a velocity of 2% c

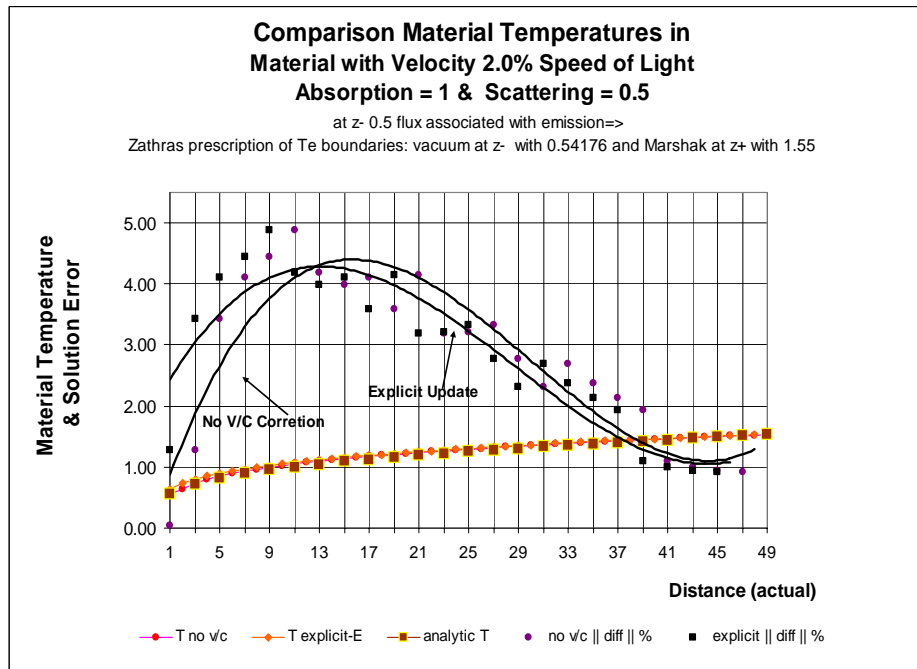


Figure 7. Comparisons of temperature as a function of depth in an absorbing and scattering material with a velocity of 2% c

The fluxes for purely absorbing media moving at 1% speed of light are shown in Figure 8. The analysis shown in Figure 8 is meant to be a self-consistent test; the differences in flux between the lab frame and the fluid's rest frame are the flux associated with material motion, the drift flux. The calculated drift flux, $\frac{4}{3}\bar{v}E$, where E is given by Planck's Law, $E = aT^4$, is shown. Also shown is the drift flux minus leakage from the vacuum boundary and drift flux plus the co-moving frame flux. These add to essentially the same values, the Eulerian flux, supplying assurance that we are calculating the Lagrangian frame flux and appropriately identifying the Eulerian frame and its flux.

At 5% the speed of light, there is a larger error than shown in Figures 3 through 7. To get a better approximation at velocities higher than 2%, we should incorporate higher-order terms in the radiative-transfer equations. The validity of the quasi-analytic solution is suspect as the velocity increases, since it too was developed by neglecting higher-order terms.

A mesh-density study was performed at 1% c for the pure absorbing case, with a grid size of 0.1mm, which is 25 times smaller than the results shown above. Approximately a 1% improvement in the solution was found near the vacuum boundary. The result was a lower material temperature and slightly less error.

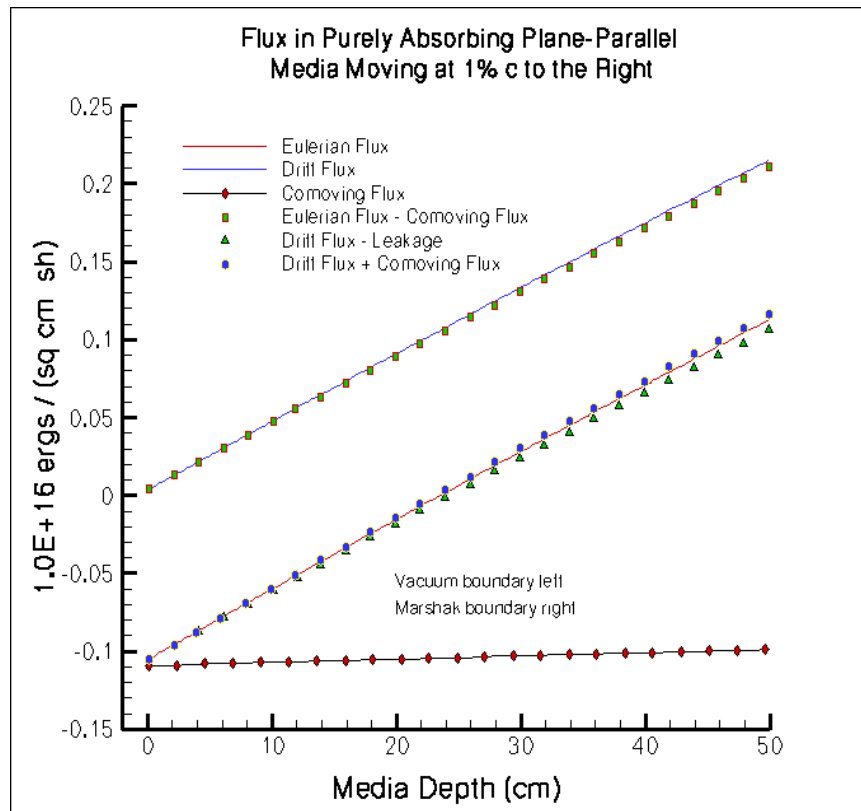


Figure 8. Comparisons of flux as a function of depth in an absorbing material with a velocity of 2% c

Conclusion

We noted good agreement up to 2% of the speed of light for the explicit-update material-motion correction formulation. The velocity-correction terms of $\mathcal{O}(v/c)$ added to the lab-frame equations mimicked slow-moving material. Utilizing faced-based values where possible in the discretization provides reasonable agreement to the transport solution for the cases studied. This approach is better than the cell-averaged correction method that we described previously (Carrington and Turner, 2004).

The explicit-update method for the energy equation shows general agreement with the quasi-analytic solution. When we considered the comparison in this study, we found it difficult to draw a conclusion about the usefulness of the correction terms. The boundary conditions for the spherical harmonic equations are determined by the quasi-analytic transport solution. The solutions are constrained to a given regime, and this situation is partly responsible for the fact that we do not have more differences between the corrected solutions and solutions without correction.

Greater differences in the energy density between methods will be found when physical processes are determining the thermo-fluid fields. When the velocity field has discontinuities or when there is a large divergence in velocity, the drift-flux term found in the divergence of the energy density flux

$$\nabla \cdot \left(\frac{\nabla E}{3} - \frac{4}{3} \bar{v} E \right) = \bar{\nabla} \cdot \frac{\bar{\nabla} E}{3} - \frac{4}{3} (E \bar{\nabla} \cdot \bar{v} + \bar{v} \bar{\nabla} \cdot E) \quad (56)$$

will have a more significant impact on the Eulerian-frame energy density.

Acknowledgments

The algorithm development in this paper was aided by conversations with Dr. Jim Morel.

Los Alamos National Laboratory (LANL), an affirmative action/equal opportunity employer, is operated by the University of California for the United States Department of Energy under contract W-7405-ENG-36. LANL strongly supports academic freedom and a researcher's right to publish; as an institution, however, the Laboratory does not endorse the viewpoint of a publication or guarantee its technical correctness.

References

- Carrington, D.B., and Turner, S.A., *Material Motion Correction for Mixed-Frame Radiative Transfer*, Los Alamos Scientific Laboratory, Los Alamos, NM, LA-UR-04-7895 (2004).
- Mihalas, D., and Klien, J.E., "On the Solution of the Time-Dependent Inertial-Frame Equation of Radiative Transfer in Moving Media to $O(v/c)$," *J. Comput. Phys.*, **46**, 97-137 (1982).

- Mihalas, D., and Mihalas, B.W., *Foundations of Radiation Hydrodynamics*, (Dover, Mineloa, N.Y., 1999), Mihalas and Weibel-Mihalas (1999).
- Knoll, D.A., Rider, W.J., and Olson, G.L., "Nonlinear Convergence, Accuracy, and Time Step Control in Nonequilibrium Radiation Diffusion," *JQSRT*, Elsevier Science Ltd., 25-36 (2001).
- Pistnner, S., and Shaviv, G., "An Analytic Solution of the Radiative Transfer Equation for a Gray Scattering Atmosphere in Motion," *The Astrophysical Journal*, **436**, 837-842 (1994).
- Mihalas, D., *Stellar Atmospheres*, 2nd Edition, (W. H. Freeman Co., 1979).
- Morel, J.E., private communication (2004).